occupied and unoccupied states of C_{60} revealed no discernible differences in the monolayer structure. For these studies, the sample bias voltages were ±(1.7 to 3.0) V and typical tunneling currents were 0.5 to 1.2 nA; images shown here for the occupied states were acquired at 1.8 to 2.2 V.

The higher resolution gray-scale STM topograph of Fig. 2a shows that C_{60} molecules form ordered arrays within large monolayer islands on GaAs(110). Despite the close-packed appearance, the ordered structure in this image does not have a hexagonal symmetry. Instead linear molecular arrays run along a direction that corresponds to the [$\bar{1}1\bar{1}$] direction of the substrate. The spacing between molecules in this direction is 9.8 Å. Figure 2b represents an image for this same surface in which linear arrays were aligned along the [$1\bar{1}\bar{1}$] direction of the substrate. Figure 2, a and b, also shows that the C_{60} molecules are bonded at different sites of the substrate, as reflected by different brightness. Lines of higher (brighter and larger) molecules, marked as B, along the above-mentioned directions are sandwiched between regular ones (marked A).

Simultaneous imaging of C_{60} islands and the adjacent substrate made it possible to determine the bonding sites of the overlayer. Figure 2c depicts the observed structure of C_{60} on GaAs(110). Two different sites, labeled A and B, correspond to open and shaded circles. The A sites, located above Ga atoms and centered on four As atoms, correspond to the darker molecules of Fig. 2a. They are ~0.8 Å lower than B sites that are centered on four Ga atoms. The difference in height reflects the intrinsic relaxation of the GaAs(110) substrate itself; that is, the outward shift of As relative to Ga as the bond rotates ~29° while retaining its bulk bond length (9). The upper part of Fig. 2a shows a single domain of A-type character with a $c(4 \times 2)$ structure with respect to the substrate. In this case, nearest neighbors of C_{60} along [$\bar{1}1\bar{1}$] or [$1\bar{1}\bar{1}$] have a separation of 9.8 Å, and those along [001] have a separation of 11.3 Å. In contrast, the lower portion of Fig. 2a reveals a domain with a mixture of A-type and B-type rows, where B-type rows can be seen as a displacement of A-type rows by 2.4 Å along the substrate [$\bar{1}1\bar{1}$] direction. Such B-type rows can also be formed by displacing A-type molecules along [$1\bar{1}\bar{1}$], as shown in Fig. 2b. The surface lattice structure of GaAs(110), shown in Fig. 2c, determines that such displacement can only produce the two configurations of A-B-A rows depicted in Fig. 2, a and b. Extended B-type domains were not observed.

These STM results demonstrate that C_{60} growth structures are determined by a bal-

ance between molecule-substrate and intermolecular interactions. A-type domains, dictated by registry with the substrate, have a compressed nearest neighbor distance of 9.8 Å, compared to 10.02 Å (1) or 10.04 Å (11) determined for closed-packed C_{60}. A remarkable molecule-substrate interaction is revealed by the facts that pure A-type domains exist in an extended area and that both A- and B-sites are essentially commensurate with the GaAs(110) substrate. Whereas previous studies of C_{60} on Au(111) showed structural instability (5), our results for GaAs(110) show much stronger interaction, with two favored sites. The stability of the C_{60} monolayer on GaAs(110) and its instability on Au(111) are most likely determined by the strength of molecule-substrate interactions. On the other hand, intermolecular interactions produce large monolayer islands that force molecules upward to B-type sites. Mixed domains with

A-sites and B-sites introduce movement out of the plane, pushing B-site molecules upward, and release stress in pure A-site domains.

REFERENCES AND NOTES

1. W. Krätschmer et al., Nature 347, 354 (1990).
2. H. W. Kroto et al., ibid. 318, 162 (1985).
3. D. L. Lichtenberger et al., Chem. Phys. Lett. 176, 203 (1991).
4. J. H. Weaver et al., Phys. Rev. Lett. 66, 1741 (1991).
5. R. J. Wilson et al., Nature 348, 621 (1990).
6. J. L. Wragg et al., ibid., p. 623.
7. R. E. Haufler et al., J. Phys. Chem. 94, 8634 (1990).
8. R. E. Haufler et al., Mat. Res. Soc. Symp. Proc., in press.
9. R. M. Feenstra et al., Phys Rev. Lett, 58, 1192 (1987).
10. Y. Z. Li et al., in preparation.
11. R. M. Fleming et al., Mat. Res. Soc. Symp. Proc., in press.
12. This work is supported by the National Science Foundation (University of Minnesota and Rice University) and the Robert A. Welch Foundation (Rice University).

The Higher Fullerenes: Isolation and Characterization of C_{76}, C_{84}, C_{90}, C_{94}, and $C_{70}O$, an Oxide of D_{5h}-C_{70}

FRANÇOIS DIEDERICH,* ROLAND ETTL, YVES RUBIN,
ROBERT L. WHETTEN, RAINER BECK, MARCOS ALVAREZ, SAMIR ANZ,
DILIP SENSHARMA, FRED WUDL, KISHAN C. KHEMANI, ANDREW KOCH

The toluene extract of the fluffy carbon material produced by resistive heating of graphite contains a variety of molecules larger than C_{60} and C_{70} in a total amount of 3 to 4% by weight. Repeated chromatography of this material on neutral alumina has led to the isolation of stable solid samples of C_{76}, C_{84}, C_{90}, and C_{94}. The characterization, which includes mass spectrometry, ^{13}C nuclear magnetic resonance, electronic absorption (ultraviolet/visible) and vibrational (infrared) spectroscopy identifies these all-carbon molecules as higher fullerenes. In addition, $C_{70}O$, a stable oxide, has been isolated that is structurally and electronically closely related to D_{5h}-C_{70}. This compound forms during the resistive heating process and probably has an oxygen atom inserted between two carbon atoms on the convex external surface of the C_{70} skeleton.

I N A SURPRISING DEVELOPMENT, Krätschmer and Huffman et al. (1) reported in 1990 the isolation of macroscopic quantities of the highly stable icosahedral-cage molecule C_{60} (buckminsterfullerene, soccer ball) (2). This new allotropic form of carbon is obtained from the benzene-soluble fraction of a fluffy soot-like material produced through resistive heating of graphite under inert atmosphere. In ad-

F. Diederich, R. Ettl, Y. Rubin, R. L. Whetten, R. Beck, M. Alvarez, S. Anz, D. Sensharma, Department of Chemistry and Biochemistry, University of California, Los Angeles, CA 90024–1569.
F. Wudl, K. C. Khemani, A. Koch, Institute for Polymers and Organic Solids, Department of Physics and Chemistry, University of California, Santa Barbara, CA 93106.

*To whom correspondence should be addressed.

dition to C_{60}, the soluble extract contains C_{70} in C_{60}:C_{70} ratios between 75:25 and 85:15 (3, 4). The two molecules, which are members of a homologous series of hollow closed-cage molecules, the fullerenes (2), are separable by sublimation (5), high-pressure liquid chromatography (HPLC) (6, 7), or liquid gravity chromatography (LC) on alumina (3, 4, 8). The predicted (2) icosahedral symmetry (point group I_h) of C_{60} has been supported by comparison of infrared (IR) and Raman spectra with theoretical predictions (1, 5), by ^{13}C nuclear magnetic resonance (^{13}C NMR) (3, 4, 9), and by scanning tunneling microscopy (STM) (10). The ^{13}C NMR data support an ellipsoidal cage shape (point group D_{5h}) for C_{70} (3, 4, 8, 11). The photophysical (12) and material properties (13) of the two fullerenes C_{60} and C_{70} as

well as their functionalization (*6*) and chemistry (*8*, *14*) are currently under extensive investigation in many laboratories. Here we report on the isolation and characterization of the larger carbon molecules C_{76}, C_{84}, C_{90}, and C_{94} and show that these compounds of yet unknown structure belong to the same family of hollow-cage molecules. In addition, the isolation of $C_{70}O$, a stable oxide of D_{5h}-C_{70} which forms during the resistive heating process, is described.

Mass spectrometric analysis of the crude benzene-extractable carbon material produced by resistive heating of graphite first suggested the presence of small quantities of larger all-carbon molecules in addition to C_{60} and C_{70}. The highly abundant ions of C_{60} ($m/z = 720$) and C_{70} ($m/z = 840$) in the spectra were accompanied by peaks of relative intensities of $\approx 10\%$ at $m/z = 914$, 1008, and 1176, indicating the presence of the all-carbon molecules C_{76}, C_{84}, and C_{98}, respectively, some properties of which had previously been considered theoretically
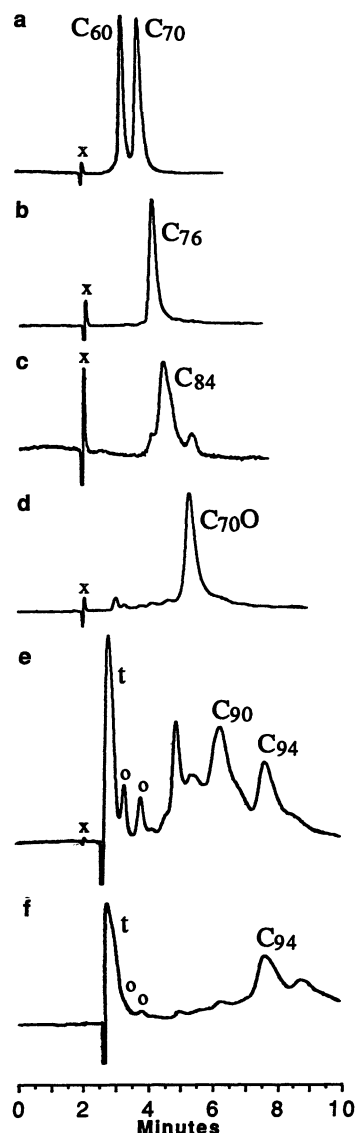

Fig. 1. HPLC profiles of the compounds isolated from the soluble carbon material produced by the method of Krätschmer and Huffman *et al.* (*1*). Experimental conditions: support, SiO₂; particle size, 5 μm; column dimensions, 24 by 0.5 cm; eluant, *n*-hexane; pressure, 1600 psi; flow rate, 2 ml/min; UV detection at 340 nm. All peak assignments are based on mass spectrometric analysis (Figs. 2 and 4). (**a**) C_{60} (retention time $t_R = 3.23$ min) and C_{70} ($t_R = 3.73$ min). (**b**) C_{76} ($t_R = 4.09$ min). (**c**) C_{84} ($t_R = 4.52$ min). (**d**) $C_{70}O$ ($t_R = 5.33$ min). (**e**) Higher fullerenes C_{90} ($t_R = 6.23$ min) and C_{94} ($t_R = 7.58$ min). (**f**) C_{94} ($t_R = 7.58$ min). For solubility reasons, toluene (2% v/v; $t_R = 2.73$ min) was added to the eluant for C_{90} and C_{94} (spectra e and f). The peaks marked "x" in spectra a to e represent a solvent impurity. The peaks marked "o" in spectra e and f correspond to residual C_{60} and C_{70} (*17*).
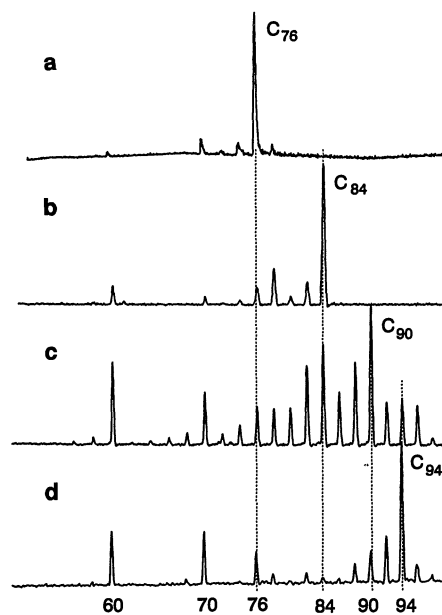
(*15*). A large improvement in the yield of produced soluble extract from initially $\approx 14\%$ (*3*) to 25 to 35% (*16*), combined with the efficiency of the gravity chromatography on alumina (*3*, *4*, *8*) in large-scale separations, enabled us to isolate and characterize the first representatives of the higher fullerenes. Starting from 500 mg of toluene-soluble extract, multiple chromatographies on neutral alumina, activity I, with hexane-toluene gradient elution (*17*) afforded, besides C_{60} and C_{70} as the major products (*8*), five dark-brown solids. These compounds, isolated in milligram quantities each (*18*), were analyzed by HPLC on silica gel (Fig. 1) and identified by mass spectrometric techniques as higher fullerenes (Fig. 2) and as the oxide $C_{70}O$. Results obtained in the separation of material from four different production runs were nearly identical.

Fast atom bombardment (FAB) and laser desorption time-of-flight (LD-TOF) mass spectrometry (*19*), both under the mildest possible conditions, were the most useful techniques for the identification of the new compounds. Electron impact (EI), desorption chemical ionization (DCI), and field desorption (FD) were not appropriate methods in this analysis. Under the conditions of these three techniques, the higher ions readily fragmented to give C_{60}^+ and C_{70}^+ as the main detectable ions. Figure 2 shows the LD-TOF spectra of the higher fullerenes. The results of FAB measurements were very similar. As a general feature in all spectra of these higher carbon ions, we note the characteristic fragmentation pattern with C_2 losses leading to C_{70}, and ultimately, to C_{60}. This fragmentation pattern has previously been observed for carbon ions generated by laser vaporization of graphite (*2*, *20*) and other carbon-rich materials (*21*). Under more drastic FAB or LD-TOF conditions, this fragmentation pattern also dominated, and C_{60}^+ and C_{70}^+ became the most intense ions among a long series of C_{2n}^+ peaks. This suggests that the most abundant fullerenes C_{60} and C_{70} may form not only directly in the resistive heating of

Fig. 2. LD-TOF mass spectra recorded for the new fullerenes. Spectrum (**a**) was obtained from the sample characterized by the HPLC profile in Fig. 1b, spectrum (**b**) from the sample characterized in Fig. 1c, spectrum (**c**) from the sample shown in Fig. 1e, and spectrum (**d**) was recorded from the sample which eluted last from alumina (Fig. 1f).

graphite but also by fragmentation of originally formed higher fullerenes. The characteristic pattern of C_2 losses seen in all mass spectra, in particular in the FAB spectra, of the higher all-carbon molecules must be considered as a strong evidence for their fullerene character.

The LD-TOF spectrum in Fig. 2a shows that the compound which gives the HPLC profile in Fig. 1b is C_{76} containing C_{78} as a minor contaminant. C_{76} and C_{78} show identical retention times by HPLC. However, C_{78} is eluted slightly more slowly on alumina, which in the entire fullerene analysis shows a remarkable molecular size discrimination. Following the initial fractions containing predominantly C_{76} (Fig. 1b) are fractions which give equal abundances of the C_{76} and C_{78} ions in the mass spectra. The ultraviolet/visible (UV/vis) spectrum of C_{76} (Fig. 3a) is distinctively different from that of C_{60} and C_{70}. The most striking feature is the new structured long-wavelength band which extends from 600 nm beyond 800 nm. The ^{13}C NMR spectrum (35,000 scans) recorded in 1,1,2,2-tetrachloroethane-d_2 in the presence of $Cr(acac)_3$ (*9*) provides additional support that C_{76} is a member of the fullerene family: a total of 16 resonances are observed in the characteristic fullerene range between 130 and 155 ppm where the signals of C_{60} and C_{70} also appear (*22*). The large number of resonances could originate either from a single compound of reduced symmetry or a mixture of C_{16} isomers.

The sample at the origin of the HPLC profile in Fig. 1c is highly enriched C_{84} as shown by the corresponding LD-TOF mass spectrum (Fig. 2b). The purity of the compound appears to be much higher by mass spectrometry than by HPLC. However, the computing integrator used for HPLC is uncalibrated, and peak intensities do not necessarily reflect product ratios. Furthermore, C_{84} could exist in the form of several constitutional isomers with similar retention times on alumina. A total of 25 resonances of similar intensity observed between 133 and 145 ppm in the ^{13}C NMR spectrum in carbon disulfide supports the presence of an isomeric mixture. Solutions of C_{84} are greenish-yellow, and the UV/vis spectrum differs from those of the other fullerenes (Fig. 3) (3). The absorption maxima (λ_{max}) of C_{84} appear in $CHCl_3$ at 280 (sh), 320 (sh), 380 (sh), 393, 476 (sh), 566, 616, 668 (sh), 760 (sh), and 912 (sh) nm. The LD-TOF mass spectrum of Fig. 2c identifies the sample shown in Fig. 1e as enriched C_{90}. The sample which elutes last from alumina (Fig. 1f) contains predominantly C_{94} (Fig. 2d).

Both FAB and LD-TOF spectra (Fig. 4) strongly suggest that the compound which gives the HPLC profile in Fig. 1d corresponds to $C_{70}O$ (m/z = 856). The intense peak in the FAB spectrum at m/z = 857 (M^+ + 1) results from hydrogen atom addition under the spectrometric condi-

tions. The major fragmentation of $C_{70}O$ leads to C_{70}. This would indicate that the oxygen atom is placed on the convex external surface of the fullerene, because an oxygen atom situated on the internal concave surface of C_{70} could not escape without destruction of the molecular framework. The oxide $C_{70}O$ is closely related to D_{5h}-C_{70}, as the oxygen atom seems to introduce only a minor structural and electronic perturbation. The UV/vis spectra of the two red solutions of C_{70} and $C_{70}O$ resemble each other in many ways (Fig. 3b). With the exception of the absence of a band at 360 nm, the spectrum of $C_{70}O$ shows all the characteristic absorptions of C_{70}, although slightly shifted and broadened. The major bands in the Fourier transform infrared (FT-IR) spectrum of C_{70} (film) at 795, 672, 641, 577, 565, and 534 cm^{-1} are also present, slightly shifted and with similar intensities, in the spectrum of a $C_{70}O$ film (796, 668, 644, 574, 561, and 527 cm^{-1}). As a result of lower symmetry, additional bands are visible in the $C_{70}O$ spectrum between 500 and 1600 cm^{-1}. No C=O band is observed; however, a strong band at 1259 cm^{-1} is assigned to an sp^2-C-O stretch in $C_{70}O$.

The oxide $C_{70}O$ is not formed during the chromatographic work-up but rather from trace oxygen impurities in the production process (23). Adsorption of pure C_{70} for

prolonged periods on alumina under exposure to air or its chromatography on this support did not yield $C_{70}O$. Since the UV/vis and IR spectra suggest that the oxygen only perturbs the C_{70} chromophore slightly, and to account for the stability of $C_{70}O$, we propose that this molecule contains the oxa-bridged [10]annulene structure (24) (Scheme I). This substructure could form in

Scheme I
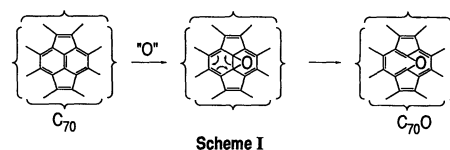
the reaction between a pyracylene unit of C_{70} with "hot" oxygen atoms present as an impurity either in the graphite or the helium gas used for the resistive heating process, or from residual traces of humidity or air in the production chamber. The oxa-bridged [10]annulene substructure in one pyracylene unit would not be expected to perturb the structural and electronic character of the residual portion of the molecule.

This preliminary investigation into the nature of higher fullerenes and functionalized derivatives will be followed by the production and separation of larger quantities of material, which should allow the complete structural characterization of these new compounds. Why are these molecules but not others, such as C_{72}, found? In contrast to the long-known and well rationalized stability of C_{60}, the basis for the relative abundances of larger carbon molecules is not at all understood, although their stability has been proposed (15) to be dependent on a confluence of structural/strain and electronic orbital-filling considerations. In addition, the present results lead to the useful working hypothesis that the extraction of the same fluffy carbon material with solvents like 1,2,4-trichlorobenzene, 1-methylnaphthalene, or pyrene and triphenylene, which are far superior to benzene and toluene in solubilizing aromatic hydrocarbons (25), should allow the isolation of fullerenes of even much higher masses (26).

Note added in proof: The extraction of 500 mg of the toluene-insoluble portion of the soot-like material with 100 ml of 1,2,4-trichlorobenzene at its boiling point (214°C) afforded after work-up ~30 mg of a black solid. Washing with toluene to remove residual C_{60} and C_{70} left 10 mg of a material which was analyzed by mass spectrometry. The FAB spectra showed a remarkably wide distribution of carbon molecules C_{2m}^+, m = 49 to 106, with the highest relative peak intensities observed between m = 58 to 68. A similar distribution is seen in the LD-TOF spectra obtained under most gentle desorption conditions.
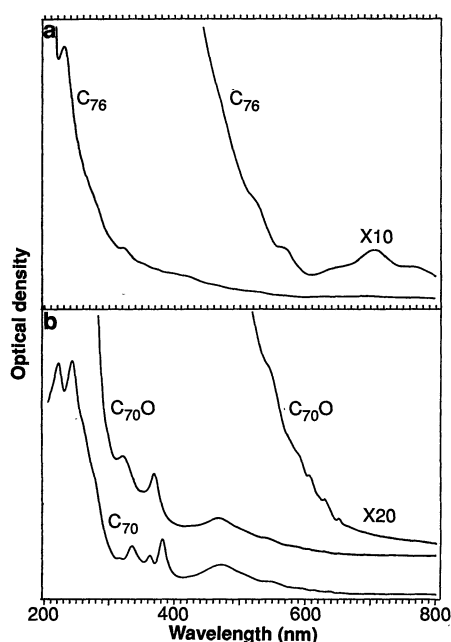

Fig. 3. UV/vis spectra recorded in n-hexane for C_{76} (**a**) and $C_{70}O$ (**b**). For comparison, the spectrum of C_{70} (3, 8) is also shown. Absorption bands for C_{76}: λ_{max} (nm) = 230, 286 (sh), 328, 350 (sh), 378 (sh), 405, 455 (sh), 528 (sh), 564, 574 (sh), 642, 709, 768. Absorption bands for $C_{70}O$: λ_{max} (nm) = 230 (sh), 258 (sh), 324, 371, 469, 540 (sh), 590 (sh), 605, 628, 650.
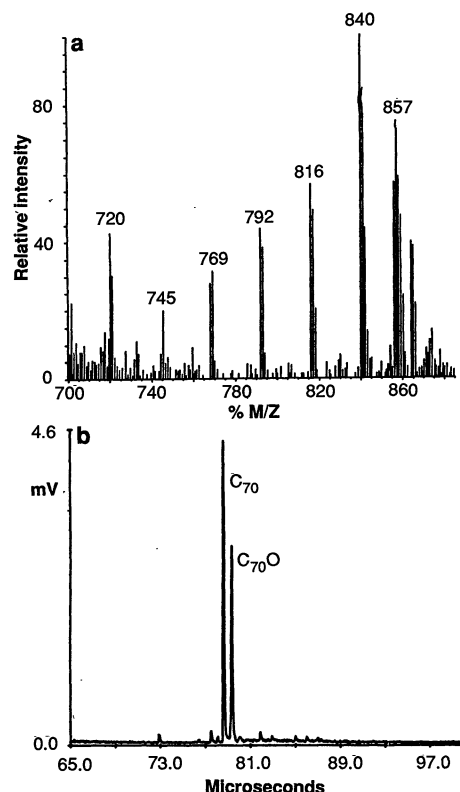

Fig. 4. (**a**) FAB (matrix: m-nitrobenzyl alcohol, discharge voltage: 3.5 kV) and (**b**) LD-TOF mass spectra of $C_{70}O$.

REFERENCES AND NOTES

1. W. Krätschmer, K. Fostiropoulos, D. R. Huffman, *Chem. Phys. Lett.* **170**, 167 (1990); W. Krätschmer *et al.*, *Nature* **347**, 354 (1990).
2. H. W. Kroto, J. R. Heath, S. C. O'Brien, R. F. Curl, R. E. Smalley, *Nature* **318**, 162 (1985); R. F. Curl and R. E. Smalley, *Science* **242**, 1017 (1988).
3. H. Ajie *et al.*, *J. Phys. Chem.* **94**, 8630 (1990).
4. R. Taylor, J. P. Hare, A. K. Abdul-Sada, H. W. Kroto, *J. Chem. Soc. Chem. Commun.* **1990**, 1423 (1990).
5. D. S. Bethune, G. Meijer, W. C. Tang, H. J. Rosen, *Chem. Phys. Lett.* **174**, 219 (1990).
6. J. M. Hawkins *et al.*, *J. Org. Chem.* **55**, 6250 (1990).
7. D. M. Cox *et al.*, *J. Am. Chem. Soc.*, in press.
8. P.-M. Allemand *et al.*, *ibid.* **113**, 1050 (1991).
9. R. D. Johnson *et al.*, *ibid.* **112**, 8983 (1990).
10. R. J. Wilson *et al.*, *Nature* **348**, 621 (1990); J. L. Wragg *et al.*, *ibid.*, p. 623.
11. R. Tycko *et al.*, *J. Phys. Chem.* **95**, 518 (1991).
12. J. W. Arbogast *et al.*, *ibid.*, p. 11.
13. P.-M. Allemand *et al.*, in preparation.
14. R. E. Haufler *et al.*, *J. Phys. Chem.* **94**, 8634 (1990).
15. P. W. Fowler, J. E. Cremona, J. I. Steer, *Theor. Chim. Acta* **73**, 1 (1988).
16. R. L. Whetten *et al.*, *Mater. Res. Soc. Symp. Proc.*, in press.
17. Details of the chromatographic separation: A total of 500 mg of carbon extract, adsorbed on 250 g of neutral alumina, activity I, was chromatographed on the same alumina using a flash chromatography column (dimensions 60 by 6.5 cm). Elution with hexane-toluene (95:5 v/v) without application of pressure gave pure C_{60}. Gradually increasing the amount of toluene from 10% to 20% and finally 50% led to the isolation of C_{70}. Flash chromatography initially with hexane-toluene (1:1, v/v) followed by mixtures with gradually higher toluene content, and finally pure toluene, afforded four yellowish mixed fractions (A to D). All four fractions were rechromatographed on neutral alumina columns (30 by 3 cm). Chromatography of fraction A with hexane-toluene (95:5 v/v) first led to the elution of residual C_{70} followed by yellow solutions of highly enriched C_{76} (Fig. 1b). The second fraction B was first chromatographed with hexane-toluene (95:5, v/v) to remove residual C_{70} and C_{76}. Increasing the amount of toluene to 7% led to the elution of C_{84} contaminated with fullerenes of higher and lower masses. A second chromatography on alumina (20 by 2 cm) afforded solutions of highly enriched C_{84} (Fig. 1c). The third fraction C was first chromatographed with hexane-toluene (85:15, v/v) to remove residual C_{76} and C_{84}. Increasing the toluene content in the eluant to 18% gave reddish solutions containing very pure $C_{70}O$ (Fig. 1d). Elution of fraction D with a toluene gradient (5 to 25%) in hexane led first to the isolation of residual C_{70}, C_{76}, and C_{84} followed by solutions containing C_{90} as the major product in addition to a lesser amount of C_{94} (Fig. 1e). Further increase in the amount of toluene afforded highly enriched C_{94} (Fig. 1f). The fullerenes C_{90} and C_{94} which were eluted with solvents of high toluene content contain C_{60} and C_{70} as minor contaminants (Figs. 1e and 1f). For solubility reasons, C_{60} and C_{70} show severe tailing during chromatography with solvents of low toluene content, and the tailing material is eluted with the toluene-rich solvents.
18. Starting from 2.5 g of toluene-soluble soot extract, chromatography as described in (17) afforded 117 mg of a mixture of the higher fullerenes containing approximately 20% of residual C_{70}, 40% of C_{76}/C_{78}, 10% of C_{84}, 10% of $C_{70}O$, 10% of C_{90} and C_{94}, and ≈10% of other fullerenes in the range between C_{70} and C_{98} as well as fullerene oxides and nitrides. From this mixture, a total of 12 mg of C_{76}, 2 mg of C_{84} and 2 mg of $C_{70}O$ was isolated in pure form. The remainder of these compounds was obtained as mixed fractions.
19. F. Diederich *et al.*, *Science* **245**, 1088 (1989); K. E. Schriver, thesis, University of California, Los Angeles (1990). Both ArF (193 nm) and Nd:YAG/4 (266 nm) lasers have been used under low-fluence

conditions (1 to 10 mJ cm^{-2}) to simultaneously evaporate and ionize solid films of the various fractions under He-jet atmosphere into a reflectron-type time-of-flight mass spectrometer.
20. E. A. Rohlfing, D. M. Cox. A. Kaldor, *J. Chem. Phys.* **81**, 3322 (1984); P. P. Radi *et al.*, *Chem. Phys. Lett.* **174**, 223 (1990).
21. H. So and C. L. Wilkins, *J. Phys. Chem.* **93**, 1184 (1989); Y. Rubin *et al.*, *J. Am. Chem. Soc.* **113**, 495 (1991).
22. ^{13}C NMR of C_{76}: δ 135.75, 142.05, 142.13, 142.87, 142.92, 143.65, 144.10, 144.20, 145.95, 146.63, 146.71, 147.28, 149.27, 150.10, 152.76, 153.17.
23. FAB mass spectra show that small amounts of the fullerene monoxides $C_{76}O$ (*m/z* = 928), $C_{84}O$ (*m/z* = 1024), $C_{90}O$ (*m/z* = 1096), and of the dioxide $C_{70}O_2$ (*m/z* =872), which were not isolated, are also formed during the resistive heating process. The formation of the trioxides $C_{72}O_3$, $C_{80}O_3$, $C_{86}O_3$, and $C_{90}O_3$, which would give the same molecular ions at unit mass resolution than the higher fullerenes C_{76}, C_{84}, C_{90}, and C_{94}, respectively, is ruled out based on the observed fragmentation patterns. In addition to the fullerene monoxides, the FAB spectra suggest the formation of the carbon nitrides $C_{76}N$ (*m/z* = 926), $C_{84}N$ (*m/z* = 1022), and $C_{90}N$ (*m/z* = 1094). The formation of the methylene derivatives $C_{77}H_2$, $C_{85}H_2$, and $C_{91}H_2$, which would show the same molecular ions at unit mass resolution, is less probable under the experimental conditions.
24. E. Vogel, M. Biskup, W. Pretzer, W. A. Böll, *Angew. Chem. Int. Ed. Engl.* **3**, 642 (1964).
25. H. A. Staab and F. Diederich, *Chem. Ber.* **116**, 3487 (1983).
26. H. Kroto, *Pure Appl. Chem.* **62**, 407 (1990).
27. Supported by the National Science Foundation (F.D., R.L.W., F.W.), the Office of Naval Research (F.D., R.L.W.), and a NATO fellowship (R.E.).

11 February 1991; accepted 8 March 1991

Deep UV Photochemistry of Chemisorbed Monolayers: Patterned Coplanar Molecular Assemblies

CHARLES S. DULCEY, JACQUE H. GEORGER, JR., VICTOR KRAUTHAMER, DAVID A. STENGER, THOMAS L. FARE, JEFFREY M. CALVERT*

Deep ultraviolet (UV) irradiation is shown to modify organosilane self-assembled monolayer (SAM) films by a photocleavage mechanism, which renders the surface amenable to further SAM modification. Patterned UV exposure creates alternating regions of intact SAM film and hydrophilic, reactive sites. The exposed regions can undergo a second chemisorption reaction to produce an assembly of SAMs in the same molecular plane with similar substrate attachment chemistry. The UV-patterned films are used as a template for selective buildup of fluorophores, metals, and biological cells.

SELF-ASSEMBLED MONOLAYER (SAM) and multilayer films are of interest for both fundamental studies and technological applications. Such films can be used in thin-film optics, sensors and transducers, protective layers, high-resolution imaging materials, and functionalized surfaces with specific chemical, biological, or adhesive properties (1–4). SAM-forming materials may be physisorbed layers, such as Langmuir-Blodgett films, or chemisorbed layers, such as organothiols bonded to Au or organosilanes bonded to silica. Both types of SAM films inherently offer a high degree of control in the direction normal to the plane of the film and substrate. Chemisorbed films are more versatile and stable, because the interaction between the film precursor and the surface is much stronger than in physisorbed films (1). However, little work has been done to control the placement of mol-

C. S. Dulcey and J. H. Georger, Jr., Geo-Centers, Inc., Fort Washington, MD 20744.
V. Krauthamer, U.S. Food and Drug Administration, Center for Devices and Radiological Health, Rockville, MD 20857.
D. A. Stenger, T. L. Fare, J. M. Calvert, Center for Bio/Molecular Science and Engineering, Code 6090, Naval Research Laboratory, Washington, DC 20375.

*To whom correspondence should be addressed.

ecules in the plane of the surface.

Two approaches for producing patterned chemisorbed SAM films have recently been reported. In one, selective surface coordination chemistry is used to bind different SAM precursors to a substrate with lithographically defined stripes of dissimilar metals (5). This approach lacks generality in that coplanar patterns of multiple SAMs with the same surface attachment chemistry cannot be produced on a substrate composed of a single material. Also, the assemblies produced by this technique are not coplanar because metal steps are typically 20 times the SAM film thickness. Alternatively, conventional lithographic processing has been used to fabricate coplanar "orthogonal" SAMs (6). Patterns of a thick polymer photoresist are defined and used to block the chemisorption of a SAM film in selected areas of the substrate. After the photoresist has been stripped, the remaining substrate is modified with a second SAM film. This technique has significant drawbacks for the formation of molecular assemblies, particularly the necessity of at least 18 processing steps.

This report describes a new approach for directly modifying and patterning SAM films by exposure to deep UV radiation.